ISEE-1 SATELLITE OBSERVATIONS OF VLF SIGNALS AND ASSOCIATED TRIGGERED EMISSIONS FROM THE SIPLE STATION TRANSMITTER

T. F. BELL, U. S. INAN and R. A. HELLIWELL

Radioscience Laboratory, Stanford University, Stanford, California 94305, U.S.A.

Abstract: During the International Magnetospheric Study (IMS), the ISEE-1 spacecraft has been an important component of VLF wave-injection experiments for studying interactions between coherent VLF waves and energetic particles. The coherent waves are injected into the magnetosphere by ground-based transmitters such as that at Siple Station, Antarctica, and those of the worldwide Omega navigation network. In this paper, we report on data acquired by the Stanford VLF receiver on ISEE-1 during the period October 1977–August 1979. The results show that the transmitter signals, propagating in the nonducted mode, are observed continuously over large regions of the plasmasphere. VLF emissions triggered by the nonducted waves generally are found to possess spectral characteristics different from those of emissions triggered by ducted signals.

1. Introduction

During the recent International Magnetospheric Study (IMS), Stanford University was involved in a number of IMS activities. Among these were:

(1) The installation and operation in 1978 and 1979 of a VLF wave direction-finder at Palmer Station, Antarctica.

(2) Participation in the International Plasmapause-Plasmasphere Dynamics Program.

(3) The conduction of controlled VLF wave-injection experiments involving the ISEE-1 spacecraft, the VLF transmitter at Siple Station, Antarctica and a VLF receiving site at Roberval, Canada.

The direction-finder (DF) study was carried out in cooperation with groups operating DF instruments in Antarctica at Halley Station (U.K.), Sanae Station (South Africa) and Belgrano Station (Argentina, France).

The International Plasmapause-Plasmasphere Dynamics Program involved plasmapause probing carried out on a campaign basis at the stations listed above, as well as at Kerguelen Island in the Indian Ocean (France) and a few other stations. Campaigns were organized on an annual basis to provide longitudinally spaced

tracking of plasmapause position and related phenomena over periods of one to two weeks in the austral winter. This work, coupled with the direction-finding, was intended to explore topics in plasmasphere dynamics that had been previously investigated from single longitudes only. Excellent data sets in both the DF area and in the general area of plasmapause probing were acquired, and the groups involved have made arrangements for data exchange and joint studies, the results of which will be available in the near future.

In the present paper, we confine our discussion to the results of the VLF wave-injection experiments carried out with the aid of the ISEE-1 satellite and the Siple Station controlled VLF transmitter. In particular, we report new observations of nonducted VLF waves from the Siple transmitter and associated VLF emissions in the magnetosphere. The data reported were acquired by the Stanford University VLF Wave Injection Experiment on the ISEE-1 satellite (BELL and HELLIWELL, 1978). The experiment has four main components: (1) a broadband (1–32 kHz) VLF receiver on ISEE-1 connected to a long electric antenna; (2) a broadband (1–20 kHz) controllable VLF transmitter located at Siple Station, Antarctica (HELLIWELL and KATSUFRAKIS, 1974); (3) various VLF navigation and communications transmitters, such as those of the worldwide Omega network; and (4) ground stations in the Antarctic and Canada. The main goal of this experiment is to study interactions between coherent VLF waves and energetic particles in the magnetosphere. Of particular interest is the whistler-mode instability through which both natural and artificially stimulated VLF emissions are produced. Sources of the coherent VLF waves involved in these studies include VLF transmitters, large-scale power grids, whistlers and other natural coherent VLF signals. The Stanford University experiment on ISEE-1 is an outgrowth of 'ground-to-ground' VLF wave-injection experiments carried out over the past five years using the Stanford University broadband transmitter at Siple Station (SI) and VLF receivers at Roberval Station (RO), the station conjugate to Siple Station (HELLIWELL and KATSUFRAKIS, 1974). However, there are a number of important differences between the ground-to-ground experiments and the 'ground-to-satellite' experiments described in the present paper.

As shown in the sketch of Fig. 1a, in a typical mode of operation of the ground-to-ground experiments VLF waves are injected into the ionosphere from a ground-based source, such as the VLF transmitter at Siple Station. A small fraction of the energy travels in ducts of enhanced ionization along paths that are closely aligned with the Earth's magnetic field. Near the magnetic equatorial plane these waves interact with energetic electrons to produce wave amplification (up to 30 dB), triggering of VLF emissions, and scattering of energetic electrons in pitch angle and energy.

The injected signals and the associated triggered emissions travel to the ionospheric region conjugate to the source and can enter the Earth-ionosphere waveguide

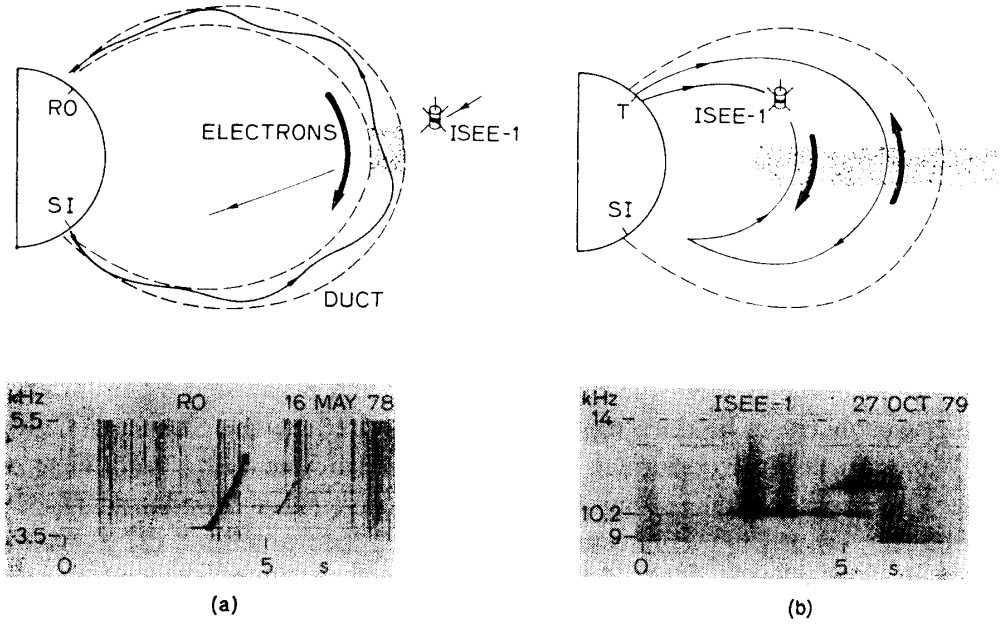

Fig. 1. Schematic representation of two classes of wave-injection experiments. (a) Siple-to-Roberval transmission through a field-aligned duct of enhanced ionization. In the interaction region (shaded) near the magnetic equatorial plane the injected waves from Siple Station (SI) interact with energetic electrons (solid arrow) to produce wave amplification, triggering of VLF emissions, and scattering of energetic electrons. A spectrogram of a typical emission triggered by a ducted wave is shown in the lower portion of the panel. (b) Ground-to-satellite transmission along nonducted paths. Both direct and indirect nonducted waves can intersect the interaction region (shown shaded), where they can interact with energetic electrons (solid arrows) to produce wave amplification, triggering of VLF emissions and energetic particle scattering. A spectrogram of a typical emission triggered by a nonducted wave is shown in the lower portion of the panel.

to be observed on the ground. A typical example of such triggered emissions is shown in the lower panel of Fig. 1a. In this example, recorded at Roberval Station (RO), a 3.6 kHz one-second-long pulse from the Siple Station transmitter triggers a strong VLF emission which rises in frequency for approximately one second at a rate of approximately 2 kHz/s.

At the end of the field line near the wave source, the scattered electrons precipitate into the ionosphere causing a variety of perturbations that can be detected from the ground. For example, fluxes of natural VLF wave-induced precipitation have been observed to excite X-rays (ROSENBERG *et al.*, 1971), photo-emissions (HELLIWELL *et al.*, 1980) and electron density enhancements (HELLIWELL *et al.*, 1973).

Although ground-based experiments can determine a number of important features of the interaction, *in situ* satellite (or rocket) measurements are required to

determine the wave and particle properties in or close to the interaction region. In addition, such measurements represent the only means of studying the class of injected waves which are nonducted. In general, most of the waves injected by a ground-based transmitter propagate in the magnetosphere in a nonducted mode. Although capable of strong interaction with energetic particles in the magnetosphere, these waves generally are internally reflected at low altitudes and do not reach the ground. Thus the only means of observing the output of wave-particle interactions involving nonducted injected waves is through the use of satellites. It is the ground-to-satellite injection experiments which are the subject of the present paper.

As shown in Fig. 1b, the nonducted waves propagate in the magnetosphere along non-field-aligned paths, usually with high wave normal angles, and can reach the satellite through a number of distinct ray paths. The nonducted waves that reach the satellite without undergoing reflection in the hemisphere conjugate to the source are termed 'direct' waves. Those that reach the satellite after either magnetospheric reflection (WALTER, 1969) or specular reflection in the hemisphere conjugate to the source are termed 'indirect' waves or 'echoes.' Although the nonducted waves are not confined to a particular field line, they can be expected to interact with energetic particles during each traversal through the interaction region, thought to lie near the magnetic equatorial plane. During some of these traversals the nonducted waves can be expected to trigger VLF emissions. A typical example of such emissions is shown in the lower panel of Fig. 1b. In this example, recorded on the ISEE-1 satellite, nonducted signals from the Omega, N.D., transmitter at 10.2 and 11–1/3 kHz trigger bursts of VLF emissions that endure for approximately three times the duration of the triggering pulses. The individual elements of each emission burst rise in frequency at a rate approaching 40 kHz/s.

During these wave-injection experiments the Stanford ISEE-1 VLF receiver determines the properties of the waves within, or near, the interaction region. The energetic particle properties are in turn measured by particle experiments also on ISEE-1. From the correlations between the wave and particle data, models for the wave amplification, emission generation and particle scattering processes are derived. In the present paper we describe only the wave phenomena observed on ISEE-1 during the wave-injection experiments. The wave-particle correlations will be described in a future study.

During the first two years of spacecraft operation the two main sources of coherent waves for the Stanford experiment have been (1) the VLF transmitter at Siple Station, Antarctica, with its precisely controlled frequency and amplitude characteristics and (2) the Omega VLF navigational transmitter located in North Dakota. With the aid of these sources the Stanford experiment has acquired data concerning nonducted coherent waves and associated triggered VLF emissions in the magnetosphere.

In this paper we present examples of nonducted coherent VLF signals from the Siple transmitter detected by ISEE-1 over large regions of the plasmasphere. We also show examples of associated emissions triggered by signals from Siple and other ground transmitters. A more detailed discussion of reception of both Siple and Omega signals, and more examples of triggered emissions, are given by BELL *et al.* (1980a).

2. Experiment Background

Fig. 2 depicts the inbound and outbound legs of typical ISEE-1 orbits near the longitude of the Siple-Roberval magnetic meridian (magnetic longitude, ϕ_m, $\sim 5°$W). Inbound and outbound legs are shown for two time periods, October 1977 (launch) and October 1979. In each case the orbits have been projected onto the appropriate meridional plane.

As shown in Fig. 2, measurements of Siple signals near or within the interaction region (magnetic equator) in the range $2 \leq L \leq 4$ were possible on the inbound leg of the ISEE-1 orbit for a few months immediately following launch on October 1977. The inclination of the ISEE-1 orbit at that time was approximately 30°, but by October 1979 the inclination had increased to 52° and the inbound leg lay far to the south of the interaction region. In this case the signals could be observed only prior to their traversal of the interaction region, and thus prior to the times of emission triggering.

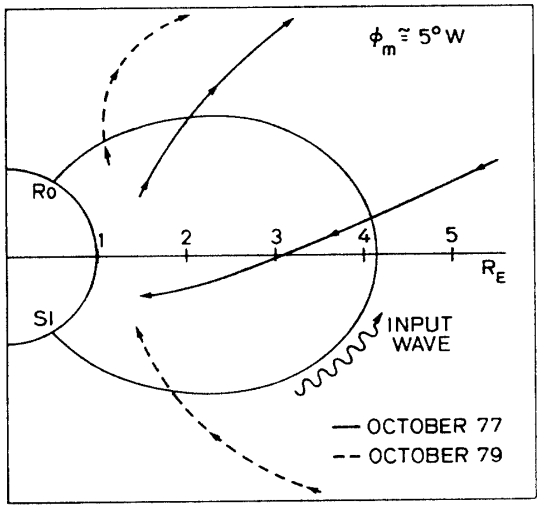

Fig. 2. ISEE-1 inbound and outbound orbits projected on the Siple-Roberval meridional plane. Orbit configurations shortly after launch (October 1977) and approximately two years after launch (October 1979) are both shown.

On the other hand, the outbound legs of the orbit during the two-year period provided data only on the output waves from the interaction region. The general character of these orbits was not a function of the inclination angle. As a consequence the data on VLF emissions triggered by nonducted Siple signals have

been obtained largely on the outbound leg of the ISEE orbit.

Partially as a result of this orbit configuration the observed incidence of VLF emission triggering by Siple signals on ISEE-1 was not as high as those triggered by other transmitter signals. Other factors contributing to this result include the transmitter output power.

During the ISEE-1 wave-injection experiments from Siple Station several transmission formats were used, examples of which are shown in Fig. 3. In general, the formats are a series of fixed-frequency pulses of variable duration, as well as frequency ramps of both positive and negative slope. Each format is designed to investigate one or more specific questions concerning the physics of the wave-particle interaction which leads to the triggering of VLF emissions. For example, the variable pulse length format shown in the upper two panels of Fig. 3 was designed to study the effect of input pulse length on the emission process (STILES and HELLIWELL, 1975) and to determine on which side of the Earth's magnetic equator the generation of rising and falling tones takes place (HELLIWELL, 1967). The 'stairstep' format also shown in these panels is designed to study the dependence of the emission process on input wave frequency and to study the wave entrainment process

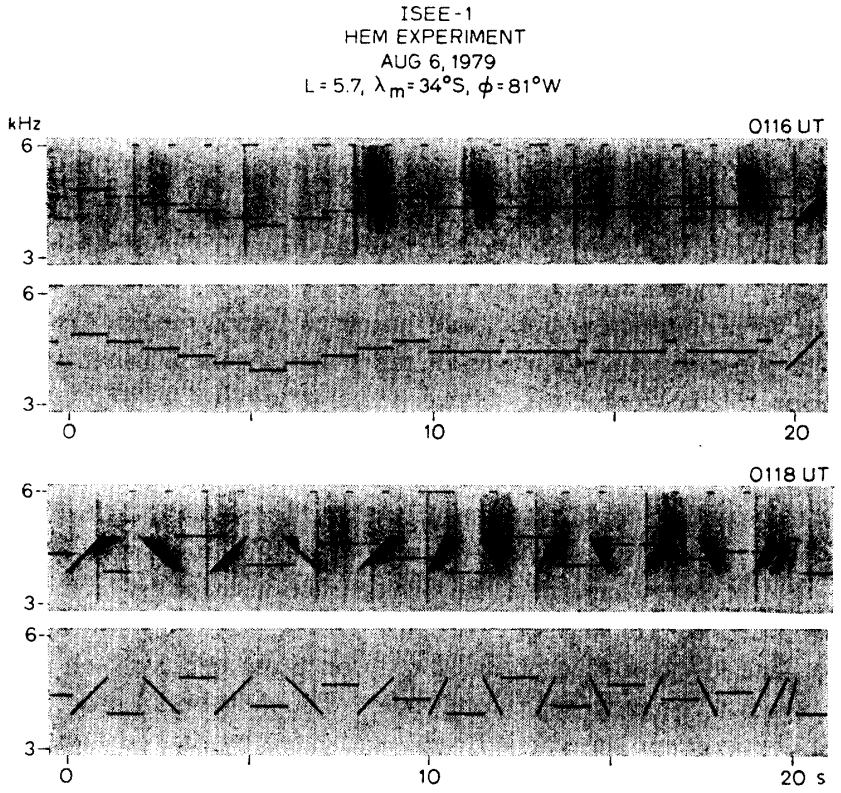

Fig. 3. Examples of transmission formats employed by the Siple transmitter and typical examples of these signals as received on the ISEE-1 satellite.

(HELLIWELL and KATSUFRAKIS, 1974) in which triggered emissions are 'captured' or entrained by subsequent transmitter pulses. Finally, the ramp format in the lower two panels is designed to study multipath effects and the effect upon the emission process of changes in the frequency of the input wave and to determine how the wave growth rate varies with the sign and magnitude of df/dt. In all formats the input wave amplitude can also be varied to show how emission generation depends on wave amplitude. Typical examples of these formats as received on the satellite are shown in the first and third panels. The formats as transmitted are shown in the second and fourth panels. Note that the received pulses are longer than the transmitted ones. This pulse elongation is produced whenever multiple paths of propagation of disparate group time delay exist between the ground and the satellite. This effect is also evident in the receptions of the frequency ramp format (third panel), where each discrete ramp of minimum time delay is seen to be followed by a diffuse distribution of a number of ramps that reach the satellite at different times.

In the following section we present data on the distribution of coherent nonducted waves in the magnetosphere and then report on some examples of triggering of VLF emissions by these waves.

3. Wave Distribution in the Magnetosphere

In this section we show that VLF signals from the Siple transmitter are detectable continuously over large regions of the plasmasphere. In addition, we show that the intensity distribution and the group time delay of the received signals are generally smooth functions of the satellite position. The smooth variation of these parameters provides strong evidence that the observed waves have propagated to the satellite in a nonducted mode, and not in a ducted mode. The widespread distribution of these nonducted waves in the magnetosphere raises the possibility that the majority of the interactions between energetic particles and coherent waves from ground-based transmitters may occur in the nonducted mode.

Fig. 4 shows a projection upon the magnetic equatorial plane of the ISEE-1 inbound orbits on which Siple transmitter signals were received during the period October 29, 1977 to August 2, 1978. Receptions during this period were typical of those during the two-year period. The orbital sections along which reception occurred are denoted by thick lines. Because of the necessity for telemetry time sharing, data generally could be obtained only on those orbits which fell within an operational 'window' in geographic longitude. The meridional range in which the wave-injection experiment was carried out is indicated by dashed radial lines at the 50°W and the 110°W longitude positions. In a simple dipole model the magnetic field lines through Siple Station intersect the magnetic equatorial plane at about $L=4.2$, longitude 75°W.

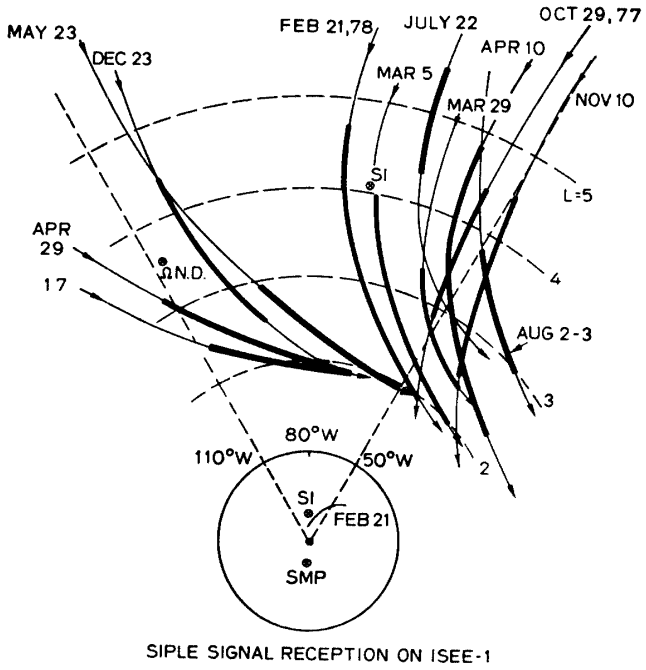

Fig. 4. Viewing area of the Siple transmitter, mapped onto the geomagnetic equatorial plane in a centered dipole system. The angular scale gives geographic longitude. Portions of the ISEE-1 orbits for the period October 29, 1977, to August 2, 1978, are shown. The heavy lines indicate the times when the transmitter signals were received on the satellite. The intersection with the equatorial plane of the magnetic field lines through the Siple and Omega transmitters are indicated by circled crosses. Points of reception of signals from the Omega, N.D., transmitter are not shown, but these signals were observed on nearly all of the portions of the orbits shown that lay in the range $1.5 < L < 4$ (see Fig. 8).

During the period indicated, Siple signals were detected on 12 of 16 orbits when transmissions were made. The transmitter signals were received mainly inside the plasmasphere, but reception was continuous over wide ranges of L-value, magnetic latitude and longitude, and the signal time delays at the satellite varied smoothly as a function of satellite position, as illustrated in Fig. 5. The 'gap' in Fig. 4 between $L=3$ and $L=5$ near the 90°W–80°W meridians is due to an absence of data for the corresponding passes for this 9-month reference period. Data from other times (*e.g.*, October–November 1978 interval) which are not shown here, indicate that Siple signals are readily detected on the spacecraft in this region. Thus there does not appear to be any unexpected longitudinal variation in the probability of reception of the Siple signals.

Sample spectrograms of the Siple signals received on ISEE-1 are shown in Fig. 6. The two panels show the received signal spectra for two different days for which the orbits are shown in Fig. 4. Note that for both days receptions at approxi-

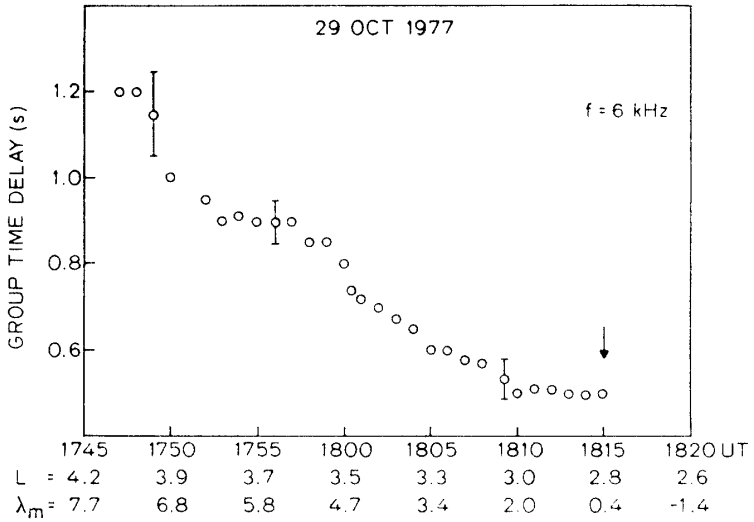

Fig. 5. Typical variation of the group time delay of Siple signals as observed on the satellite, shown for one of the orbits of Fig. 4. The smooth variation of the signal time delays is an indication that the observed signals are nonducted.

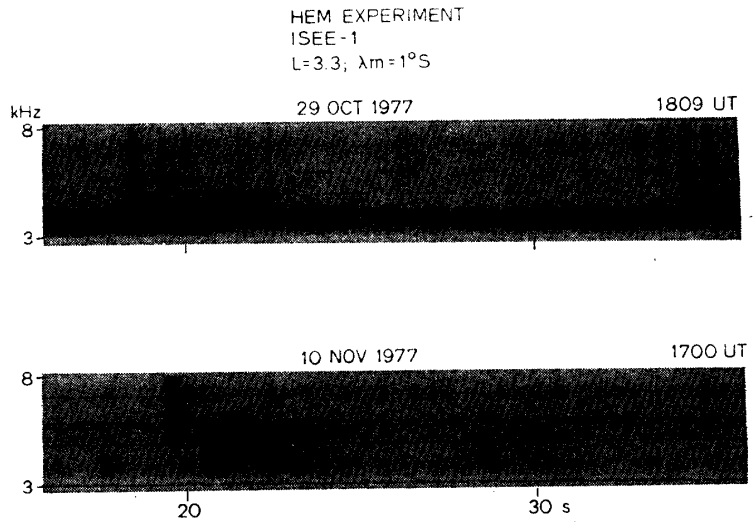

Fig. 6. VLF spectrograms of typical Siple transmitter signals observed on ISEE-1 for two of the orbits of Fig. 4. The two panels show receptions on different days but at approximately the same location in space. The transmitted frequency-time format is identical in both cases. The upper panel shows well-defined pulses of standard length, indicating the existence of but a single ray path from the ground to the satellite. The lower panel shows another day with prominent multipath and/or echoing effects. Note that individual pulses are virtually indistinguishable, indicating that the signals reach the satellite on various paths with group time delay differences of up to ~2 seconds. In the lower panel the line near 7 kHz is due to onboard interference from another experiment.

mately the same location in space are shown. The transmitted frequency-time format is identical in both cases. In the upper panel the individual transmitter pulses are easily distinguished since on this day there apparently was only one ray path available from the ground to the satellite. The reception of the same format on a day when multipath and/or echoing effects were prominent is shown on the lower panel. In this case the pulses are not distinguishable, indicating that the signals reached the satellite through various paths with group time delay differences of up to ~ 2 seconds. The reception shown in this lower panel occurred at a time of unusually quiet activity ($Kp \sim 0$). Data received on this day are described in detail in another report (BELL *et al.*, 1980b).

As indicated in the introduction, most of the transmitter signals observed on the ISEE-1 satellite are believed to propagate to the satellite along non-field-aligned, *i.e.*, nonducted, paths. This belief is predicated upon present knowledge of the cross-sectional dimensions of whistler ducts. These ducts are believed to consist of field-aligned enhancements of ionization which have lateral dimensions of $\lesssim 1000$ km near the magnetic equatorial plane (ANGERAMI, 1970). Thus, if the received signals were ducted, the signals should fade in and out as the satellite traverses these irregularities. Since a typical satellite velocity is ~ 5 km/s, one would then expect to see fluctuations of a few minutes' period in the received signal amplitude when the satellite orbit is transverse to the field lines. Furthermore, since whistler ducts are believed to occupy less than 10% of the inner magnetosphere, any continuous reception of the signal for periods longer than a few minutes would be improbable. However, as indicated in Fig. 4, the transmitter signals are received continuously over a distance of a few L-shells and for times up to one hour.

Additional evidence for the nonducted character of the signals is provided by the fact that the group time delay of the received signals was observed to vary smoothly as would be expected from a distribution of nonducted rays reaching the satellite. An example of this feature is shown in Fig. 5, where the group time delay is plotted versus time for the same day represented by data in the upper panel of Fig. 6. The signal time delay varied smoothly over a period of ~ 30 minutes, or over a distance of ~ 8000 km. The presence of ducted waves in the data would be manifested in a sharp decrease in time delay of 0.3 to 0.5 s for an interval of a few minutes. No such decrease is evident.

The amplitude of the Siple signals as measured on the ISEE-1 spacecraft varied over a range of ~ 40 dB. The higher amplitudes were usually recorded on those orbits which passed close to the Siple-Roberval meridian. The data from one such orbit is displayed in Fig. 7, where the one-minute average of the wave electric field amplitude is plotted as a function of time, L-shell, magnetic latitude and longitude. The higher amplitudes for $L > 3$ correspond to times when the southern foot of the field line passing through the satellite was within 500 km of the transmitter. The type of slow amplitude change shown here as a function of L-shell is typical of

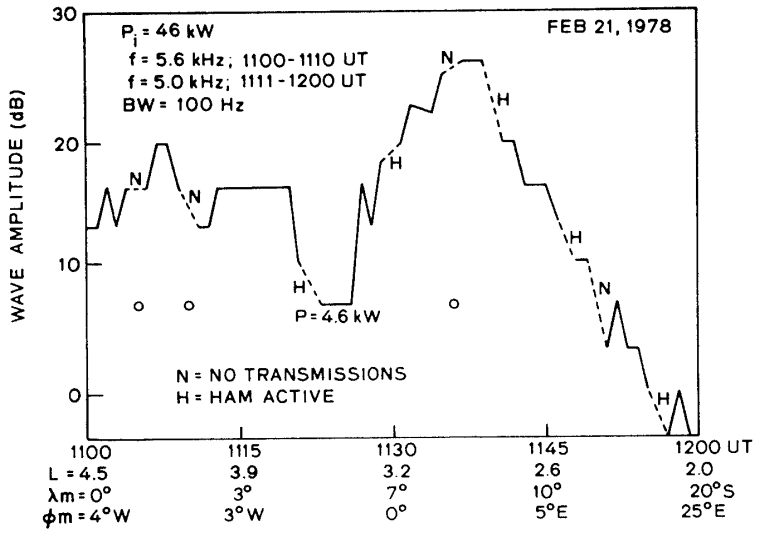

Fig. 7. The amplitude variation of the Siple signals received on ISEE-1 on February 21, 1978. The amplitude is measured in a 100-Hz band centered on the transmitter frequency. The 0 dB level corresponds to an absolute electric field intensity of ~0.1 μV/m. The southern foot of the field line passing through the satellite is indicated on Fig. 4. The solid lines indicate periods where the signal was received; the dashed lines indicate periods where either no transmissions were made or strong interference from another experiment (HAM) caused the receiver to saturate. The background noise level during periods of no transmissions is indicated by circles directly beneath the dashed portions. The reduction in intensity in the interval 1120–1125 UT is due to a deliberate 10 dB reduction in the transmitter radiated power in this period. The L-value, and geomagnetic latitude (λ_m) and longitude (ϕ_m), are also shown.

Siple signals received inside the plasmasphere on ISEE-1 and provides further support for the idea that the received signals propagate mainly in the nonducted mode.

The absolute intensities given in Fig. 7 are subject to an error of as much as 10 dB, due to a malfunction of the housekeeping circuitry which monitors the envelope of the received signal wave form. A joint study is presently underway with the University of Iowa experimenters on ISEE-1 (GURNETT *et al.*, 1978) to recalibrate the Stanford experiment and to refine the amplitude values given in Fig. 7.

4. Triggered VLF Emissions

In this section we present examples of artificially stimulated VLF emissions observed on the ISEE-1 satellite.

The number of observed cases of VLF emissions triggered by Siple signals has been lower than those triggered by signals from the Omega, N.D., transmitter. Two main reasons for this were (1) the ISEE-1 orbit was more favorable for ob-

serving the Omega signals at the output of the interaction region, and (2) the relatively higher (10: 1) radiated power of the Omega transmitter. Numerous examples of emissions triggered by the Omega transmitter signals are given in BELL *et al.* (1980a). Most of these emissions appeared to be triggered when the waves were propagating in the nonducted mode and the emissions displayed different spectral characteristics from those generally associated with emissions triggered by ducted signals. Furthermore, the path selectivity characteristics of the emission process was different in the case of triggering by nonducted waves (BELL *et al.*, 1980a).

An example of these triggered emissions is shown in the two panels of Fig. 8. The data samples of the two panels are four minutes apart in time and are representative of receptions during a period of triggering that lasted ~10 min. It should be noted here that the transmission format of the Omega, N.D., transmitter consists of a repeated train of pulses of 0.9–1.2 s duration transmitted without overlap at distinct frequencies of 10.2, 11.05, 11–1/3, 13.1 and 13.6 kHz. The repetition period of the train of pulses is 10 s. Note from Fig. 8 that the duration of each received pulse at 10.2 kHz is approximately 3 s, indicating that there exists

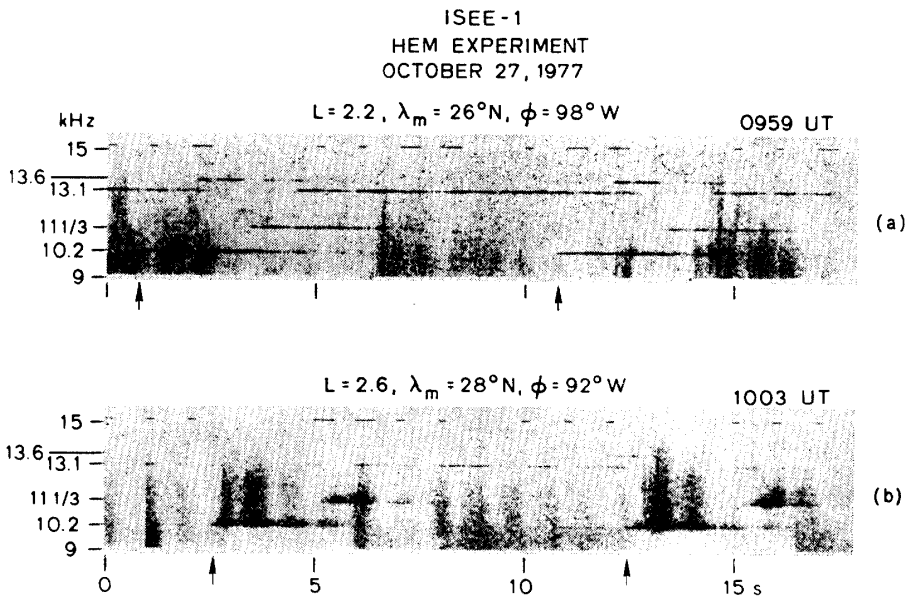

Fig. 8. Omega, N.D., signals and associated emissions received during the triggering event of October 27, 1977, as the satellite moved outward from L=2.2 (0959 UT) to L=2.8 (1005 UT). The Kp value at this time was 3⁺ and satellite local time was ~0400 UT. (a) Beginning of the triggering event, where arrows on the time axis indicate the instant at which the 'direct' pulses reach the satellite; (b) intense noise bursts triggered by the Omega signals. The intensity modulation with ~1-s period is caused by the spin of the satellite (see text). Arrows here indicate the arrival of the echo and associated emissions.

more than one path of propagation from the ground to the satellite. Superposition of a number of pulses arriving at different times produces the elongated pulses of ~3 s duration. Fig. 8a shows the wave spectrum at the beginning of the event. Arrows along the time axis indicate the instant at which the strong direct pulses at 10.2 kHz reach the satellite. The echoes (later-arriving pulses) and emissions arrive approximately one second later, producing a continuous signal of approximately 4 s duration. At this time the emissions consist of short rising tones of small bandwidth and relatively low intensity.

The situation is reversed a few minutes later, as shown in Fig. 8b. Here the amplitude of the direct pulses at 10.2 and 11–1/3 kHz is only slightly above the noise level, whereas the echoes are strong and trigger intense multi-emission noise bursts. Arrows along the time axis indicate the arrival time of the echo and associated emissions. The time delay between the direct pulse and the echo pulse is ~2 s. The emissions consist of discrete tones which rise rapidly in frequency across a 5-kHz band above the transmitter frequency. The rate of change of frequency of these rising tones approaches 40 kHz/s, a value much larger than the ~1–10 kHz/s rate for natural emissions observed on the ground (presumably ducted) (ALLCOCK and MOUNTJOY, 1970) and natural emissions observed outside the plasmasphere (BURTIS and HELLIWELL, 1976). The discrete nature of the rising tones is obscured because of the large number of emissions triggered by the echo; thus they appear noise-like in character.

Spin modulation of ~1-s period is seen in the amplitude of the triggered noise bursts in Fig. 8 and in the background noise near the 10-s mark. This modulation occurs at half the spin period of the satellite and results from the non-uniform excitation of the dipole antenna as it rotates in the wave field.

An example of emissions triggered by Siple transmitter signals is shown in Fig. 9; they are representative of a ~15-min period during which Siple signals were observed on ISEE-1. As shown in the figure, the transmitter pulses were occasionally observed to trigger very intense noise bursts. The upper panel shows a Siple pulse at 5.8 kHz triggering a very intense burst of rising emissions. The beginning of the triggering pulse is indicated by an arrow. Following this event a second, less intense noise burst is triggered by a Siple pulse at 5.6 kHz. The lower panel shows a one-second pulse at 5.6 kHz triggering two intense rising emissions and a weak hook-like tone which oscillates in frequency for a short time and apparently triggers a second intense noise burst consisting of multiple rising tones.

These triggering events were observed at a time when the satellite was located in the northern hemisphere on a magnetic shell outside the plasmapause at $L \approx 9$. At such a location direct field-aligned propagation to the satellite is not possible since the equatorial gyrofrequency on this L-shell is less than the transmitter frequency. One possibility is that the received signal reached the satellite after reflection from the ionosphere. The measured group delay is ~1 second, indicating

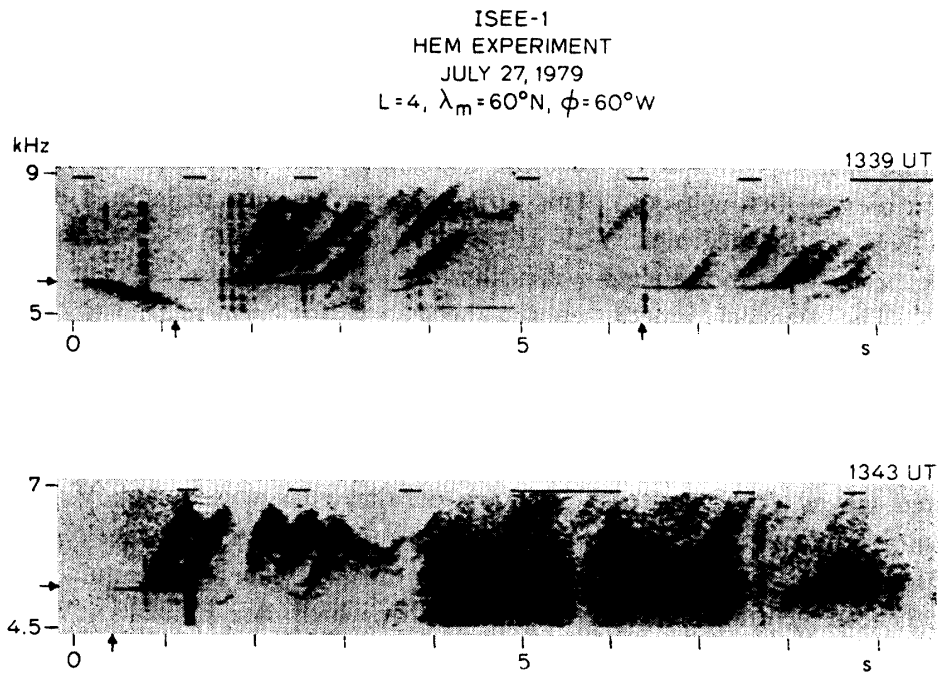

Fig. 9. Emissions triggered by Siple transmitter signals and observed on ISEE-1 on July 27, 1979. The data shown are representative of the observations during 1327–1344 UT when the satellite moved outwards from L=6.4 to L=9.6 at $\lambda_m \simeq 60°N$. The Kp index for this time was 3 and the satellite local time was in the range ~0900–1100 UT. Note that emissions were triggered by whistlers and other natural signals as well as the Siple transmitter pulses. The locations of the transmitter pulses that are clearly triggering emissions are indicated by arrows on both the time and frequency axes.

that propagation into the northern hemisphere took place in a region of relatively low plasma density. Thus, there is reason to believe that these triggering events occurred outside the plasmapause. This hypothesis is supported by raytracing calculations which indicate that propagation to the satellite location is possible only if the signal is incident on the ionosphere at a location that is poleward of a large-scale horizontal gradient in plasma density. In this context, the unusual nature of the triggered emissions may be a result of the triggering having taken place outside the plasmapause. In fact, the intense burst-like structure of the emissions in Fig. 9 resembles the structure of emissions triggered by ducted whistlers propagating just outside the plasmapause (CARPENTER, 1978).

5. Discussion and Conclusions

Our study has revealed important differences between the spectra of triggered VLF emissions observed on a high-altitude satellite and those observed on the ground. First, the satellite emissions usually consist of intense multi-emission

noise bursts of large bandwidth. Furthermore, the maximum time rate of change of frequency of the individual emissions in these noise bursts is often as much as three times higher than that of emissions triggered by ducted waves.

Second, emissions triggered by nonducted coherent waves are regularly observed on magnetic shells as low as $L=2$, while those triggered by ducted waves are not generally observed below $L=3$. This difference may be due to lack of data concerning low L-shells since most VLF ground stations lie at $L \gtrsim 3$; or the difference may arise because the nonducted waves interact with a different class of energetic electrons. The parallel kinetic energy necessary for non-relativistic electron gyroresonance with 10.2-kHz waves near the magnetic equator at $L=2$, assuming a cold plasma density of $N_0 \simeq 4000\ \mathrm{cm}^{-3}$, is given approximately by

$$E_{\|} \simeq 90\ (\cos\theta)^{-1}\ \mathrm{keV}\ . \tag{1}$$

For ducted waves, $\theta \sim 0$ and the necessary parallel energy is ~ 90 keV. On the other hand, if the cold plasma near the $L=2$ magnetic shell is in a state of diffusive equilibrium, it can be shown that the wave normal angle for nonducted waves exceeds 65° near the magnetic equatorial plane, for which case $E_{\|} > 200$ keV. Thus, nonducted waves should interact with higher energy, quasi-relativistic electrons and the pitch angle distribution of these particles during disturbed times could conceivably be more favorable for the emission generation process. The fact that nonducted coherent signals can interact with inner radiation belt particles lends further credence to the suggestion that certain anomalies discovered in the pitch angle distribution of energetic electrons might be due to gyroresonance interactions in the magnetosphere with coherent VLF signals from ground transmitters (VAMPOLA and KUCK, 1978).

It is instructive to compare our satellite results on nonducted waves with previous work on ducted signals observed on the ground. CARPENTER and MILLER (1976) showed that during the 1973–1974 time period Siple signals were detected at Roberval on approximately 20% of the days on which signals were transmitted (72 out of 374 days). During periods of reception the average Kp was $\simeq 2$. Approximately 80% of the signals observed at Roberval were determined to have propagated along magnetic shells in the range $3.5 < L < 4.5$ and none of the observed signals was found to have propagated on magnetic shells of L-values less than 3 or greater than 5.

In our own study of nonducted waves we have found that for those times when ISEE-1 was within the plasmasphere at a longitude within 30° of the transmitter location, the probability of observing Siple and Omega signals was $\sim 50\%$ and $\sim 80\%$, respectively. Thus the nonducted transmitter signals were observed on ISEE-1 much more frequently than ducted Siple signals were observed at Roberval. This result agrees well with a previous study of satellite reception of nonducted signals from the Siple transmitter (INAN *et al.*, 1977).

There are at least two reasons for the higher probability of reception on satellites. First, ground stations such as Roberval must rely upon the presence of active whistler ducts near the station in order to guide the magnetospheric signals into the Earth-ionosphere waveguide, from where they can propagate to the receiver. If ducts are not present at any particular time, the nonducted signals will suffer internal reflection in the ionosphere and will not reach the ground station. Second, the duct endpoint must lie within approximately 300 km of the receiver location or else the signals will suffer too much attenuation in the Earth-ionosphere waveguide and will generally not be observed (CARPENTER and MILLER, 1976). The stringency of these conditions for reception of ducted signals precludes a high detection probability.

We conclude that nonducted signals from low-powered VLF transmitters, such as that at Siple Station, can illuminate large regions of the magnetosphere. Within these regions these signals can interact strongly with energetic electrons to produce VLF emissions under much more general conditions than previously reported.

Acknowledgements

We wish to acknowledge valuable discussions with D. L. CARPENTER, J. P. KATSUFRAKIS and C. G. PARK concerning the ISEE-1 data. Thanks also to K. DEAN for final preparation of the typescript. This work was supported by the National Aeronautics and Space Administration under contract NAS5-20871.

References

ALLCOCK, G. McK. and MOUNTJOY, J. C. (1970): Dynamic spectral characteristics of chorus at a middle-latitude station. J. Geophys. Res., **75**, 2503–2510.

ANGERAMI, J. J. (1970): Whistler duct properties deduced from VLF observations made on the Ogo 3 satellite near the magnetic equator. J. Geophys. Res., **75**, 6115–6135.

BELL, T. F. and HELLIWELL, R. A. (1978): The Stanford University VLF wave injection experiment on the ISEE-A spacecraft. IEEE Trans. Geosci. Electron., **GE-16**, 248.

BELL, T. F., INAN, U. S. and HELLIWELL, R. A. (1980a): Nonducted coherent VLF waves and associated triggered emissions observed on the ISEE-1 spacecraft. Submitted to J. Geophys. Res.

BELL, T. F., LUETTE, J. P. and INAN, U. S. (1980b): ISEE-1 observations of VLF line radiation in the earth's magnetosphere. In preparation for J. Geophys. Res.

BURTIS, W. J. and HELLIWELL, R. A. (1976): Magnetospheric chorus: Occurrence patterns and normalized frequency. Planet. Space Sci., **24**, 1007–1024.

CARPENTER, D. L. (1978): Whistlers and VLF noises propagating just outside the plasmapause. J. Geophys. Res., **83**, 45–57.

CARPENTER, D. L. and MILLER, T. R. (1976): Ducted magnetospheric propagation of signals from the Siple, Antarctica, VLF transmitter. J. Geophys. Res., **81**, 2692–2700.

GURNETT, D. A., SCARF, F. L., FREDRICKS, R. W. and SMITH, E. J. (1978): The ISEE-1 and ISEE-2 plasma wave investigation. IEEE Trans. Geosci. Electron., **GE-16**, 225.

HELLIWELL, R. A. (1967): A theory of discrete VLF emissions from the magnetosphere. J.

Geophys. Res., **72**, 4773–4790.

HELLIWELL. R. A., KATSUFRAKIS, J. P. and TRIMPI, M. L. (1973): Whistler-induced amplitude perturbation in VLF propagation. J. Geophys. Res., **78**, 4679–4688.

HELLIWELL, R. A., MENDE, S. B., DOOLITTLE, J. H., ARMSTRONG, W. C. and CARPENTER, D. L. (1980): Correlations between λ4278 optical emissions and VLF wave events observed at $L \sim 4$ in the Antarctic. To be published in J. Geophys. Res., **85**.

HELLIWELL, R. A. and KATSUFRAKIS, J. P. (1974): VLF wave injection into the magnetosphere from Siple Station, Antarctica. J. Geophys. Res., **79**, 2511–2518.

INAN, U. S., BELL, T. F., CARPENTER, D. L. and ANDERSON, R. R. (1977): Explorer 45 and Imp 6 observations in the magnetosphere of injected waves from the Siple Station VLF transmitter. J. Geophys. Res., **82**, 1177–1187.

ROSENBERG, T. J., HELLIWELL, R. A. and KATSUFRAKIS, J. P. (1971): Electron precipitation associated with discrete very-low-frequency emissions. J. Geophys. Res., **76**, 8445–8452.

STILES, G. S. and HELLIWELL, R. A. (1975): Frequency-time behavior of artificially stimulated VLF emissions. J. Geophys. Res., **80**, 608–618.

VAMPOLA, A. L. and KUCK, G. A. (1978): Induced precipitation of inner zone electrons. 1. Observations. J. Geophys. Res., **83**, 2543–2551.

(Received April 16, 1980)